

# Nanoscale

Accepted Manuscript



This is an *Accepted Manuscript*, which has been through the Royal Society of Chemistry peer review process and has been accepted for publication.

*Accepted Manuscripts* are published online shortly after acceptance, before technical editing, formatting and proof reading. Using this free service, authors can make their results available to the community, in citable form, before we publish the edited article. We will replace this *Accepted Manuscript* with the edited and formatted *Advance Article* as soon as it is available.

You can find more information about *Accepted Manuscripts* in the [Information for Authors](#).

Please note that technical editing may introduce minor changes to the text and/or graphics, which may alter content. The journal's standard [Terms & Conditions](#) and the [Ethical guidelines](#) still apply. In no event shall the Royal Society of Chemistry be held responsible for any errors or omissions in this *Accepted Manuscript* or any consequences arising from the use of any information it contains.

## ARTICLE

# Nano-ceramic support materials for low temperature fuel cell catalysts

Cite this: DOI: 10.1039/x0xx00000x

Haifeng Lv, Shichun Mu\*

Received 00th January 2012,  
Accepted 00th January 2012

DOI: 10.1039/x0xx00000x

www.rsc.org/

Low temperature fuel cells (LTFCs) have been received broad attention due to their low operating temperature, virtually zero emissions, high power density and efficiency. However, the limited stability of the catalysts is the critical limitation to the large scale commercialization of LTFCs. In the state of art, carbon supports undergo corrosion under the harsh chemical and electrochemical oxidation conditions, which results in the performance degradation of the catalysts. Therefore, non-carbon materials with high oxidation resistant under strongly oxidizing conditions of LTFCs are the ideal alternative supports. This perspective highlights the advances and scenarios in using nano-ceramic as the supports to enhance the stability of the catalysts, the solutions to improve the electrical conductivity of nano-ceramic materials, and the synergistic effects between metal catalyst and support to help improve the catalytic activity and CO/SO<sub>2</sub> tolerance of the catalysts.

## 1 Introduction

As one of the important low temperature fuel cells (LTFCs), proton exchange membrane fuel cells (PEMFCs) are promising future devices used for portable electronics, transportation and emergency electric power sources because of environmentally friendly and highly efficient energy conversion [1-10]. A typical fuel cell device that a fuel (usually hydrogen) is converted into electricity at the anode, the oxygen is reduced at the cathode at the same time. In general, the platinum nanoparticles (Pt NPs) on carbon (Pt/C) catalysts are the most widely used to catalyze the reaction. However, the low stability is a still critical limitation to the wide spread commercialization of PEMFCs [11-13]. In currently catalytic studies, Pt and its alloy NPs have been the high active catalysts for the hydrogen oxidation reaction (HOR) at the anode and the oxygen reduction reaction (ORR) at the cathode in PEMFCs [14-19]. Unfortunately, these Pt-based NPs are unstable under such chemical and electrochemical oxidation conditions. The corrosive environment results in a decrease in the electrochemical surface area (ECSA) because of the Pt NPs migration/aggregation, dissolution/redeposition (Oswald ripening process), and detachment due to the support corrosion [20-23]. Meanwhile, even trace amounts of carbon monoxide (CO) presented in the reformat H<sub>2</sub>/CO and sulfur (e.g., SO<sub>2</sub>) in air are prone to poison the surface of Pt NPs and substantially increases the overpotential for HOR (0.7 V) or ORR [24-28]. As a result, tremendous efforts have been made toward the development of the high-performance catalysts with enhanced durability and CO/SO<sub>2</sub> tolerance in recent years [29-31].

So far, several approaches have been successfully developed to improve the catalytic performance and utilization efficiency of Pt catalysts. Different types of Pt-based nanostructure, such as nanowires (NWs), nanotubes, nanospheres, and nanofibers, have been reported as the alternative catalysts to replace the traditional Pt/C catalysts [32-36]. The novel ultrathin Pt monolayer shell-Pd nanowire core catalysts show excellent ORR activity and electrochemical stability under accelerated half-cell testing condition as compared with the commercial Pt NPs [37]. On the other hand, the traditional carbon black support (e.g., Vulcan XC-72), with high surface area, good electric conductivity and high porosity, has a low standard electrode potential (0.207 V vs reversible hydrogen electrode (RHE)) for the complete oxidation of carbon to CO<sub>2</sub>, leading to being unstable under the harsh chemical and electrochemical oxidation conditions at the cathode during fuel cell operation. A series of researches have been devoted to develop the novel supports with long-term stability. More stable nanostructure carbon, such as graphene nanosheets, carbon nanotubes, and carbon nanofibers, have been employed as catalyst supports, because their high degree of graphitized structure provides a higher resistance to chemical and electrochemical oxidation [38-44]. For instance, FePt NPs have been assembled on the graphene as catalysts for ORR, and shown that the novel catalyst are stable under the ORR conditions and show nearly no activity change after 10,000 potential sweeps between 0.4 and 0.8 V [45]. Despite tremendous efforts, the carbon oxidation also occurs in using these carbon-based materials as the catalyst supports at elevated potential due to the low standard corrosion potential for carbon. Therefore, noncarbon

materials with high oxidation resistant and stability are needed most urgently.

More recently, nano-ceramic materials have attracted much attention to increase the durability of the Pt catalysts due to their unique mechanical properties, excellent thermal stability, and outstanding oxidation and acid corrosion resistance. The typical CVs for the nano-ZrO<sub>2</sub> ceramic and carbon black supports before and after oxidation treatment at 1.2 V held for 48 h are showed in Figure 1. It can be seen that the ceramic has almost no change in the redox region after oxidation treatment for 48 h at 1.2 V, which means there are negligible surface oxides (Figure 1a). In contrast, a visible current peak occurs in the redox region for carbon black (Figure 1b), which results from the surface oxide formation due to the hydroquinone-quinone (HQ-Q) redox couple on the carbon black surface. These results indicate that the ceramic material is more corrosion resistant and durable when used in fuel cells. Some metal oxides, carbides and nitrides have been found to facilitate the increment of the stability for the Pt-based NPs when supported on such supports. Although the ceramic supports greatly improve the stability of the catalysts, the universal low electrical conductivity of ceramic is the main issue to limit their commercialization in fuel cells [46-49]. This work highlights the recent advances and research prospect in using nano-ceramic as the supports to enhance the stability of the catalysts, the solutions to improve the electrical conductivity of nano-ceramic materials, and the synergistic effects between metal catalyst and support to help improve the activity and CO/SO<sub>2</sub> tolerance of the catalysts. The nano-ceramic materials have been proven to be a promising solution to address the stability of the metal catalysts, not only for fuel cells, and even for broader industrial fields.

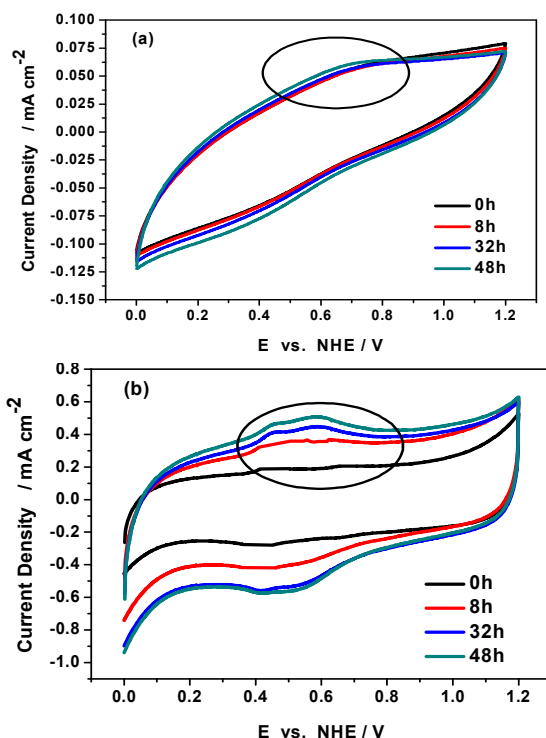


**Figure 1** Typical CV curves of ceramic (ZrO<sub>2</sub>) (A) and carbon supports (Vulcan XC-72) (B) by held at 1.20 V (versus RHE) for different durations (0.5 M H<sub>2</sub>SO<sub>4</sub>, scan rate: 20 mV s<sup>-1</sup>, temperature: 25 °C). Reproduced from Ref. 112, Copyright the Royal Society of Chemistry 2012

## 2 Improve the stability of the catalysts by employing electrochemically inert ceramics

Nano-ceramic materials are usually used as the stable supports due to their excellent resistance to the electrochemical oxidation and acid corrosion in the fuel cell environment. Metal oxides, nitrides, borides and carbides show potential application prospect in replacing the traditional carbon black supports, which can improve the stability of the metal NPs catalysts. Several representative ceramic supports used to enhance the stability of the catalysts will be mentioned in this perspective.

### 2.1 Conducting Metal Oxides

Ti<sub>n</sub>O<sub>2n-1</sub> (where n is between 4 and 10) is widely used in fields of photocatalysis, water splitting, and gas sensors. Recently, Ti<sub>n</sub>O<sub>2n-1</sub> has shown promising effects on the durability and catalytic activity of fuel cell catalysts because of its good mechanical resistance and stability in acidic and oxidative environments. Among this series of distinct oxides, Ti<sub>4</sub>O<sub>7</sub> exhibits the highest electrical conductivity exceeding 10<sup>3</sup> S cm<sup>-1</sup> at 25 °C [50-53]. Ioroi et al. studied the catalytic activity and stability of the Pt NPs on Ti<sub>4</sub>O<sub>7</sub>, which was prepared by reduction of TiO<sub>2</sub> powder at high temperature [52]. Before testing the electrocatalytic activity of the Pt/Ti<sub>4</sub>O<sub>7</sub> catalysts, the stability of the Ti<sub>4</sub>O<sub>7</sub> support was compared with that of the conventional carbon black support. The onset potential of the corrosion current during the positive direction sweep of CV was much higher for Ti<sub>4</sub>O<sub>7</sub> than that for the carbon black, indicates that Ti<sub>4</sub>O<sub>7</sub> has higher resistance to the electrochemical oxidation than the carbon black. The Pt/Ti<sub>4</sub>O<sub>7</sub> also exhibited good activity for both HOR and ORR compared to the conventional Pt/C catalyst. Moreover, it showed greater stability than the conventional Pt/C catalyst at high-potentials (1h holding at 1.0-1.5 V vs anode). So the Pt/Ti<sub>4</sub>O<sub>7</sub> catalyst is potential as both the corrosion-resistant anode and cathode catalysts for fuel cells.

Popov et al. [54] synthesized a novel TiO<sub>2</sub>-supported Pt electrocatalyst and compared the fuel cell performance with that of the Pt/C catalyst, although TiO<sub>2</sub> had low electrical conductivity [55-57]. The Pt/TiO<sub>2</sub> catalysts exhibited excellent fuel cell performance as well as ultrahigh stability at high positive potentials, which was attributed to the low mass transport limitation in the cathode catalyst layer. Figure 2 shows the polarization curves for the Pt/TiO<sub>2</sub> electrocatalysts after the potential was held at 1.2 V for 0-200 h and the normalized ECSA of the two electrocatalysts as a function of T<sub>c</sub>. The polarization curves were similar even after a corrosion time (T<sub>c</sub>) of 200 h, in contrast the Pt/C catalyst as a benchmark showed a more decrease in performance (93% after T<sub>c</sub>=80 h) due to the corrosion of carbon support and the induced

migration and agglomeration of Pt NPs at high positive potentials. The ultrahigh stability of the Pt/TiO<sub>2</sub> catalyst can be attributed to a strong metal support interaction between the Pt NPs and the TiO<sub>2</sub> support synthesized via a template-assisted route. It has been reported that TiO<sub>2</sub> can anchor the Pt NPs by interacting with Pt, thereby inhibit Pt migration and agglomeration.

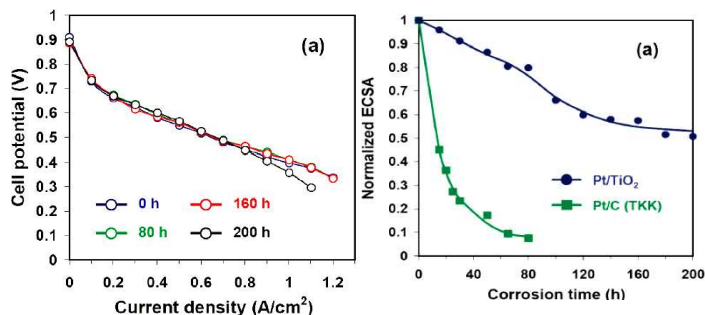


**Figure 2** (a) Polarization curves for PEMFCs with Pt/TiO<sub>2</sub> electrocatalysts after the potential was held according to the accelerated stress test protocol for 0-200 and 0-80 h, respectively. The Pt loading was 0.5 mg cm<sup>-2</sup> on the anodic side (LT140EW, BASF) and 0.4 mg cm<sup>-2</sup> on the cathodic side. (b) Normalized electrochemical surface area as a function of corrosion time for Pt/TiO<sub>2</sub> and Pt/C electrocatalysts. Reproduced with permission from ref. 54. Copyright the American Chemical Society 2009.

Tin oxide (SnO<sub>2</sub>) is a transition-metal dioxide with rutile structures, which is usually applied as oxygen deficient n-type semiconductor [58-60]. The SnO<sub>2</sub> was also prepared as a catalyst support due to its unique electrical, chemical, and physical properties [61-63]. The Pt/SnO<sub>2</sub> catalyst exhibited good electrochemical activity for ORR and much better stability in CV cycling tests (up to 1.3 V) when compared with the Pt/C. Surprisingly, after 1000 cycles the ECSA loss of the Pt/C was nearly 90%, whereas the Pt/SnO<sub>2</sub> only approached a maximum of 50% ECSA after 5000 cycles. Meanwhile, the Pt/C catalyst showed a dramatic increase in the average particle size of Pt NPs. In contrast, slight agglomeration was observed for the Pt/SnO<sub>2</sub> due to the strong interaction between Pt NPs and tin oxide [64].

Other metal oxides, such as SiO<sub>2</sub>, WO<sub>x</sub> and ZrO<sub>2</sub>, were also reported as the potential stable supports for the fuel cell catalysts due to their specific properties [65-75].

## 2.2 Metal nitrides

Resembling metal oxides, nano-metal nitrides (e.g., ZrN, TiN, TaN, VN) also have attracted much attention owing to their excellent thermal and chemical stabilities and possessing some potential catalytic properties that are similar to those of noble metals. Among them, titanium nitride (TiN) is widely used as the alternative supports for fuel cell catalysts until now. TiN is a triple bond transition metal compound which is chemically inert, has outstanding oxidation and acid corrosion resistance, and higher electrical conductivity (4000 S m<sup>-1</sup> as opposed to

1190 S m<sup>-1</sup> for carbon black) [76-78]. These specific properties make it an excellent candidate for the durable fuel cell catalyst support replacing carbon. Haldar et al. [79] synthesized the Pt/TiN catalyst via a polyol process, which showed higher electrochemical performance than the conventional Pt/C catalyst under PEMFC conditions. The TiN support is electrochemically inert and functions as a good electrical conductor in the potential region. The prepared Pt/TiN has similar ECSA to the Pt/C and higher ORR activity for the Pt/TiN was also exhibited in comparison with the carbon supported catalyst. The stability of TiN under fuel cell conditions has also been studied [80, 81]. The TiN NPs supports had a lower corrosion rate compared to the conventional carbon black, and an active behavior of TiN NPs can be observed in sulphuric acid electrolyte at 60 °C, due to the formation of -OH groups on their surface which reduce the electrical conductivity thereby inhibiting the electron transportation property. The derogation mechanism of the Pt/TiN is also different with the Pt/C catalysts. As the same amount of Pt NPs was loaded on both supports, unlike the Pt/C, which undergoes degradation via carbon corrosion and Pt NPs agglomeration mechanism, the Pt/TiN electrocatalyst degrades solely via surface agglomeration of Pt NPs [79-81].

In addition, the non-metal nanonitrides, such as BN and Si<sub>3</sub>N<sub>4</sub>, also own the good thermal and chemical stabilities [82, 83], which are worth considering in application as stable catalyst supports.

## 2.3 Titanium diboride (TiB<sub>2</sub>)

TiB<sub>2</sub> is another relatively new titanium based support which has been considered as the base material for a range of technological applications. TiB<sub>2</sub> ceramic obtains many superior properties, including high melting point, great hardness, good electrical, high thermal conductivity, excellent thermal stability and corrosion resistance in acidic medium [84,85]. In 2010, for the first time, our group reported the TiB<sub>2</sub> as a stable support for fuel cell catalysts [86]. The TiB<sub>2</sub> powders prepared by self-propagating high-temperature synthesis (SHS), were uniform, and had a narrow size distribution. The Pt/TiB<sub>2</sub> was prepared by a colloid route, and the highly dispersed Pt NPs were stabilized by Nafion functional polymer, which significantly facilitates the dispersion of Pt NPs on the TiB<sub>2</sub>. An improvement of ORR activity was observed in terms of onset potential. The Pt/TiB<sub>2</sub> showed a higher reduced current density of 0.29 mA cm<sup>-2</sup> at 0.9 V as compared to the Pt/C (0.11 mA cm<sup>-2</sup> at 0.9 V) with the same Pt loading, because the SO<sub>3</sub><sup>-</sup> end groups in the polyelectrolyte chain structure of Nafion can facilitate the reaction species transfer process for ORR. Further, it was found that the electrochemical stability of the Pt/TiB<sub>2</sub> catalyst is about four times higher than that of the Pt/C under electrochemical oxidation cycles in the potential range of 0.6-1.2 V. The perfluorosulfonic acid serving as both a proton-conducting polymer and a stabilizer was also employed to coat the surface of TiB<sub>2</sub> before depositing Pt NPs [87]. The Pt/TiB<sub>2</sub> was much more stable than that of the Pt/C, which is attributed to the excellent stability of the TiB<sub>2</sub> support and the

stabilization effect of Nafion. The above studies show a scenario for the TiB<sub>2</sub> ceramic as an alternative support for the fuel cell catalyst.

The other stable nano-metal boride ceramics, including ZrB<sub>2</sub>, MB<sub>6</sub> (M=Ca, Ba, Sr, La, etc.) have been reported [88-90]. Among them, ZrB<sub>2</sub> possesses a metal-like electric conductivity and a high resistance against wear and oxidation [91], which is most promising in fuel cell catalyst supports.

### 3 Improve the electric conductivity of ceramics by hybridizing supports

The nano-ceramic supports possess the excellent resistance to electrochemical oxidation and stability in acidic, which properties recommend consideration of the nano-ceramic as the alternative catalyst support. However, the low electrical conductivity of some ceramic materials may prevent their extensively applied in fuel cells, because of its negative effects on the catalytic activity. Therefore, it is of importance to develop new nano-ceramic supports, which not only can enhance the electrochemical stability of the catalysts, but can improve the catalytic performance of the catalysts. Therefore, the hybridized support systems combining nano-ceramic and carbon supports or doping metal elements into the nano-ceramic supports have been developed.

#### 3.1 Hybrid supports by introducing carbon

Carbon can also be introduced into the ceramic supports-based catalysts by physically combined method, to improve the catalytic activity by increasing the electrical conductivity. Silicon carbide (SiC) is a popular material with many desirable properties, including high thermal conductivity, and stability in acidic and oxidative environments [92-94]. However, the low electrical conductivity of the nano-SiC prevents its application in fuel cell catalyst supports. Although, Pt NPs were homogeneously dispersed on the surface of the SiC supports with a particle size of about 3 nm [95], the low ECSA (12 m<sup>2</sup> g<sup>-1</sup>) of the Pt/SiC was not in accordance with the more homogenous dispersion of Pt NPs. After the carbon was introduced into the Pt/SiC, the ECSA the Pt/SiC/C catalysts greatly increased to 48 m<sup>2</sup> g<sup>-1</sup> with a comparable ECSA to that of the Pt/C (62 m<sup>2</sup> g<sup>-1</sup>). This indicates that the poor electrical conductivity of nano-ceramic materials can be greatly improved by adding carbon. This hybrid catalyst also showed the higher stability than that of the Pt/C due to the excellent stability of the SiC support. There was only 8.9% of the initial ECSA of Pt/C remained, whereas 22.5% of the initial ECSA of Pt/SiC/C remained after 4000 cycles. In addition, such catalyst, with the similar ORR activity to the Pt/C catalysts, showed a higher stability of the ORR than that of the latter, which was remarkably consistent with the ECSA loss as mentioned above. Therefore, the addition of carbon in a ceramic supported catalyst supplies a possibility to synthesize an advance catalyst with high electrocatalytic performance and stability.

In order to further improve the electrical conductivity of nano-SiC, the SiC@C core shell structure support was developed for fuel cell catalysts. The SiC@C was prepared by graphitization of nano-SiC using a vacuum annealing treatment, and then the Pt NPs were dispersed on the SiC@C hybrid support via a microwave-assisted reduction method. The Pt/SiC@C catalysts exhibited higher stability and much better catalytic activities for methanol oxidation reaction (MOR) and ORR than in comparison to the conventional Pt/C catalysts [96]. Morgen et al. [97] also synthesized the high electrical conductivity nano-SiC supports using nano-porous carbon black as a template. The novel nano-SiC based catalysts show a higher catalytic activity than that of the conventional Pt/C catalysts, which open up a new era of nano-SiC ceramic for the fuel cell catalyst supports.

Further, the electrical conductivity and activity of the catalyst can be further enhanced using advanced nano-carbon materials (e.g., graphene, carbon nanotube/nanofibers) or optimizing architectures between the nano-ceramic and the nano-carbon [98, 99]. Song et al. reported the Ultra-long Pt nanolawns supported on TiO<sub>2</sub>-coated carbon nanofibers as 3D hybrid catalyst for methanol oxidation, which showed the great potential as the active anode in direct methanol fuel cells (DMFCs) [99].

#### 3.2 Hybrid supports by doping metal element

Titanium oxides are the alternative support materials for fuel cell catalysts have been mentioned above due to their good mechanical resistance and stability in acidic and oxidative environments [100-102]. However, their universal low electrical conductivity prevents their practical application in fuel cell catalysts. Different elements, such as vanadium (V), niobium (Nb), and tantalum (Ta), have been introduced into TiO<sub>2</sub> to help improve the electrical conductivity. Among them, Nb is the most promising dopant because of the similarity of the ionic radii between Nb<sup>5+</sup> and Ti<sup>4+</sup> results in almost no lattice distortion [103-105]. Popov et al. reported the rutile phase Nb-doped titanium oxide (Nb<sub>x</sub>Ti<sub>(1-x)</sub>O<sub>2</sub>) as a cathode catalyst support and investigated their stability and activity in fuel cell condition [106]. The Pt/Nb<sub>x</sub>Ti<sub>(1-x)</sub>O<sub>2</sub> catalyst showed comparable ORR activity to that of the Pt/C. The Pt/C lost 96% of its initial activity (from 3.18 to 0.13 mA cm<sup>-2</sup>) at 0.85 V after 2500 linear potential cycles, whereas there was only 59% lost for the Pt/Nb<sub>x</sub>Ti<sub>(1-x)</sub>O<sub>2</sub>. Meanwhile, the Pt/Nb<sub>x</sub>Ti<sub>(1-x)</sub>O<sub>2</sub> showed nearly ten-fold higher ORR activity than Pt/C catalyst after the potential cycling experiment. Fuel cell testing showed that the Pt/Nb<sub>x</sub>Ti<sub>(1-x)</sub>O<sub>2</sub>-based had only a small voltage loss after 3000 cycles. In contrast, there was no activity remained for the conventional Pt/C catalyst after 1000 cycles because of severe oxidation of carbon and subsequent disintegration of the catalyst layer. The experiment demonstrated that the Nb doped Nb<sub>x</sub>Ti<sub>(1-x)</sub>O<sub>2</sub> supports is a new hopeful approach to improve the performance and durability of the fuel cell catalysts.

ITO is a degenerated crystalline structure semiconductor with a wide band gap, and formed by substitutional doping of In<sub>2</sub>O<sub>3</sub> with Sn which replace In<sup>3+</sup> atoms in the cubic bixbyite structure

of indium oxide. ITO also possesses the special qualities of optically transparent and electrically conductive, which has been long used as transparent electrodes in organic light emitting diodes and solar cells [107-109]. Chhina et al., for the first time, reported the effects of catalytic activity and stability of Pt/ITO using ITO as the catalyst support [110]. Pt/ITO catalysts were prepared via reflux method, which Pt NPs were dispersed on commercially available ITO, and both the thermal and electrochemical stability were compared with that of conventional Pt/C catalysts. The crystallite sizes calculated from XRD were 38 nm and 13 nm for ITO and Pt NPs, respectively. The Pt/ITO presented a significantly enhanced stability over the Pt/C after the oxidation cycle between +0.6 and +1.8 V, and hydrogen desorption peaks in the CVs existed even after 100 cycles for the Pt/ITO. In contrast, most of the active surface area was lost after 100 cycles for the Pt/C, which indicates that the ITO support catalyst has a lower ECSA loss under accelerated voltage cycling.

Recently, Mustain et al. reported that ITO NPs were conceived as a high catalytic activity and durability support for the Pt NPs [111]. To prepare ITO NPs, the indium acetylacetonate ( $\text{In}(\text{acac})_3$ ) and tin bis-(acetylacetonate) dichloride ( $\text{Sn}(\text{acac})_2\text{Cl}_2$ ) with variable ratios were decomposed in oleylamine at 250 °C for 3 h. Pt NPs were deposited on the surface of the ITO through galvanic displacement of Cu by Pt. The ECSA of Pt was determined to be 83.1  $\text{m}^2 \text{g}^{-1}$  for Pt/ITO, which was about three times that of the Pt/C (27.3  $\text{m}^2 \text{g}^{-1}$ ). The electron transfer number was calculated to be about 3.9 at 0.6-0.85 V from the slopes of Koutecky-Levich plots, illustrating a 4e<sup>-</sup> oxygen reduction process. The Pt/ITO catalyst had a ORR specific activity of 0.750  $\text{mA cm}^2$  at 0.9 V, which was 3 times higher than that of the Pt/C (0.235  $\text{mA cm}^2$ ). On the other hand, after normalization to the loading amount of Pt metal, the mass activity of the Pt/ITO was about 4 times higher than that of the Pt/C (Figure 3). The higher catalytic activity of the Pt/ITO is likely caused by synergistic effects between the surface Sn of ITO and the supported Pt NPs. The stability of both Pt/ITO and the conventional Pt/C was investigated by applying potential sweeps at the rate of 10 mV/s to a thin-film rotating disk electrode in an O<sub>2</sub>-saturated 0.1 M HClO<sub>4</sub>. The half-wave potential of the Pt/ITO showed only a cathodic shift of approximately 4 mV in the mixed kinetic diffusion controlled region after 1000 cycles. In comparison, the shift in the half-wave potential for Pt/C was 20 mV. After the stability test, the Pt/ITO showed almost no recordable loss of Pt ECSA. In contrast, the Pt/C catalyst retained only 65% of the initial ECSA after the potential cycling. Therefore, ITO has potential as oxidation-resistant candidate materials as catalyst supports in PEMFCs.

### 3.3 Hybrid supports by introducing nano-ceramics into carbon supports

Recently, our group developed a novel strategy to improve the stability of the Pt/C catalyst using a zirconia (ZrO<sub>2</sub>)-carbon hybrid as the Pt NPs support. The hybrid support not only showed the excellent stability of ceramic supports, but showed

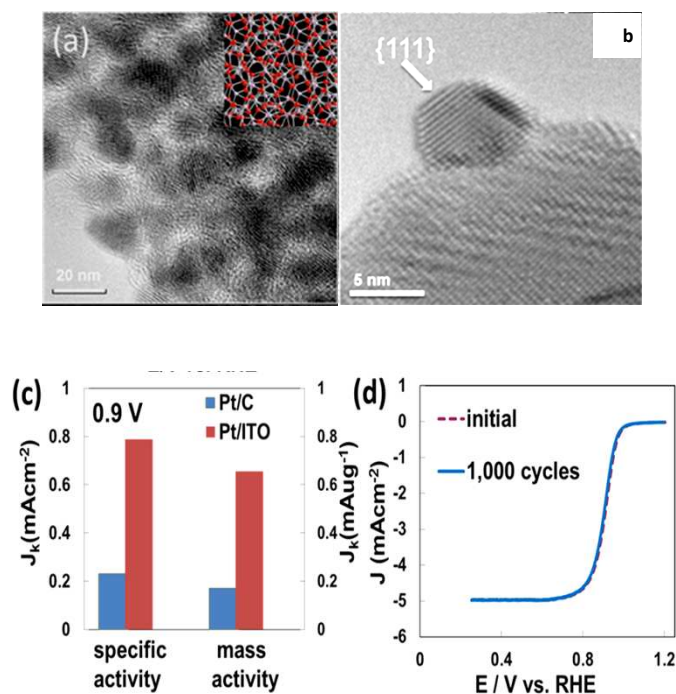


**Figure 3** TEM images of tin-doped indium oxide NPs: (a) unheated 5atom %, inset shows an uncrystallized structure; (b) HRTEM image of Pt NP supported on ITO prepared by heating to 500 °C, 5 atom %. (c) Mass activity and specific activity at 0.9 V vs RHE for Pt/ITO and Pt/C. Mass and specific activities are given as kinetic current densities ( $j_k$ ) normalized in reference to the loading amount and ECSA of metal, respectively. (d) Polarization curves for the O<sub>2</sub> reduction reaction on Pt/ITO catalysts on a rotating disk electrode, before and after 1000 cycles. Sweep rate, 10  $\text{mV s}^{-1}$ ; rotating rate, 1600 rpm. Reproduced with permission from ref. 111. Copyright the American Chemical Society 2013.

the superior electrical conductivity of carbon supports [112]. For the Pt/ZrO<sub>2</sub>-C, firstly the Pt/C catalyst was synthesized through an ethylene glycol reduction method, and then the nano-ZrO<sub>2</sub> shell with excellent thermal, chemical and electrochemical stability was introduced into the Pt/C by isothermal hydrolysis of the ZrOCl<sub>2</sub>·8H<sub>2</sub>O aqueous solution at low temperature. The nano-ZrO<sub>2</sub> shell not only can inhibit the migration and aggregation of the Pt NPs by inhabiting the undecorated surface of the carbon supports, but can dramatically protect the carbon support from chemical and electrochemical corrosion. After 2500 cycles, the Pt/C catalysts retained only 14% of the initial ECSA (from 63 to 9  $\text{m}^2 \text{g}^{-1}$ ). Although some loss of ECSA (from 51 to 22  $\text{m}^2 \text{g}^{-1}$ ) on Pt/ZrO<sub>2</sub>-C was observed, the Pt/ZrO<sub>2</sub>-C showed higher retention (41%) of ECSA compared with the Pt/C. On the other hand, the ORR activities of both the Pt/ZrO<sub>2</sub>-C and Pt/C catalysts were similar, illustrating a very limited impact of ZrO<sub>2</sub> on the catalytic activity of Pt NPs catalysts. This work represents a novel and significant strategy to functionalize the nanocatalyst support with remarkably high stability which has great potential application in fuel cells.

The Pd/ZrC-C and Pd/ZrO<sub>2</sub>-C catalysts with zirconium compounds ZrC or ZrO<sub>2</sub> and carbon hybrids as novel supports for formic acid fuel cell catalysts have also been reported [113]. They showed higher activity and stability than that of the Pd/C catalyst for formic acid electrooxidation because of the inherently excellent mechanical resistance of zirconium compounds (ZrC and ZrO<sub>2</sub>), and metal-support interaction. Similarly, the TiC-C and TiO<sub>2</sub>-C hybrid materials as the Pd NPs supports for the formic acid electrooxidation were also been reported [114]. The addition of Ti compounds significantly increased the catalytic and stability of Pd NPs for formic acid electrooxidation due to the outstanding oxidation, acid corrosion resistance of TiC and TiO<sub>2</sub> supports and the synergistic effect between Pd NPs and supports.

Wang et al. firstly grew ITO NPs on functionalized graphene sheets to form an ITO-graphene hybrid and studied their application as catalyst supports [115]. Pt-ITO-graphene was synthesized via the polyol processes. DFT calculations were also conducted to understand the preferential bonding of Pt NPs with both graphene support and ITO NPs at the triple junction points, and also suggested that the defects and functional groups on graphene help improve the stability of the catalysts. The stability of the catalysts was measured by continuously applying linear potential sweeps. As can be seen in Figure 4, there was only 14 mV degradation in half-wave potential for the Pt-ITO-graphene after potential sweeps; In contrast, the Pt-graphene revealed a remarkable negative shift 40 mV degradation. The ECSA of both catalysts also was calculated before and after ADT, and its loss of Pt-graphene was 62%, whereas the Pt-ITO-graphene only degraded 45%. As respected, these results were remarkably consistent with the ORR activity results. This study developed a new approach to combine the metal catalyst, metal oxide, and carbon materials.

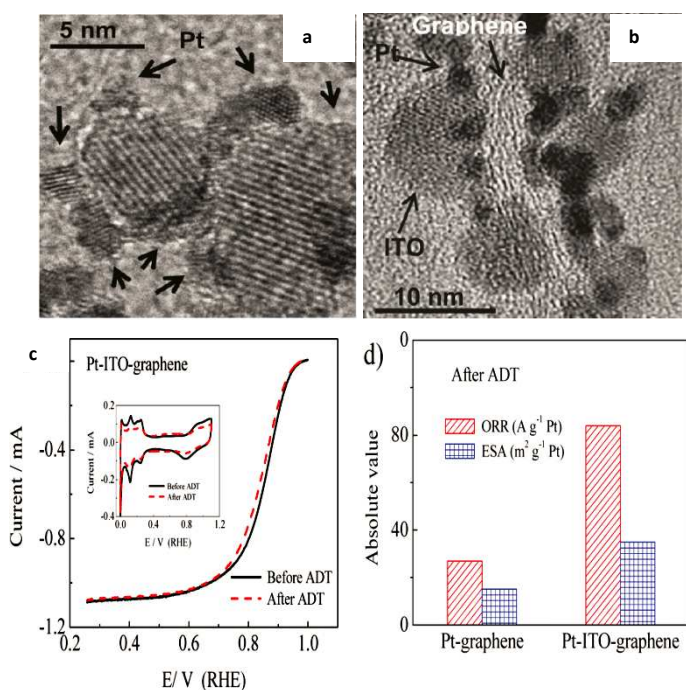


**Figure 4** TEM images (a and b) of Pt-ITO-graphene triple-junction nanostructures; Linear sweep voltammometry polarization curves of oxygen reduction on Pt-ITO-graphene (c) and Pt-graphene (d) in O<sub>2</sub>-saturated 0.1 M HClO<sub>4</sub> (5 mV s<sup>-1</sup>, 1600 rpm). Inset: Cyclic voltammograms on Pt-ITO-graphene and Pt-graphene in N<sub>2</sub>-saturated 0.1 M HClO<sub>4</sub> (50 mV s<sup>-1</sup>). Reproduced with permission from ref. 115. Copyright the American Chemical Society 2011.

#### 4 Improve the catalytic activity by synergistic effects

The nano-ceramic supports can not only improve the stability of the catalysts but can enhance the catalytic activity and CO/SO<sub>2</sub> poisoning resistance of the catalysts by the synergistic effects between the metal catalyst and the nano-ceramic supports.

##### 4.1 Improve the ORR activity

Shen et al. reported the bimetallic carbide Co<sub>6</sub>Mo<sub>6</sub>C<sub>2</sub> supported on graphitic carbon (Co<sub>6</sub>Mo<sub>6</sub>C<sub>2</sub>/<sup>g</sup>C), prepared by an anion-exchange method, and further used it as the supports of Pt NPs [116]. The Pt-Co<sub>6</sub>Mo<sub>6</sub>C<sub>2</sub>/<sup>g</sup>C catalyst showed higher ORR activity in comparison with the Pt/C catalyst. Its half-wave potential exhibited a significant positive shift of 80 mV than that of the Pt/C, which indicates that such support promotes the ORR kinetics due to the synergistic effect between the Co<sub>6</sub>Mo<sub>6</sub>C<sub>2</sub> support and active Pt NPs. Meanwhile, the catalyst exhibited 271.7 A g<sub>pt</sub><sup>-1</sup> at 0.9 V, which was 2.5 times higher than that of the Pt/C (108.6A g<sub>pt</sub><sup>-1</sup>). Also, the higher stability than that of the Pt/C catalysts after the linear sweeping cycles, was found. There was only a 6 mV shift negative for the catalyst in the half-wave potential, while the degradation of 27 mV was observed for the Pt/C catalyst (Figure 5). With the similar synergistic effect, the Pd/WC-Mo<sub>2</sub>C/C was prepared and showed a superior activity for the ethylene glycol (EG) oxidation, which is almost ten times higher than that of the Pd/C. The above findings indicate that the bimetallic transition-metal carbide can be the potential supports for fuel cell catalysts.

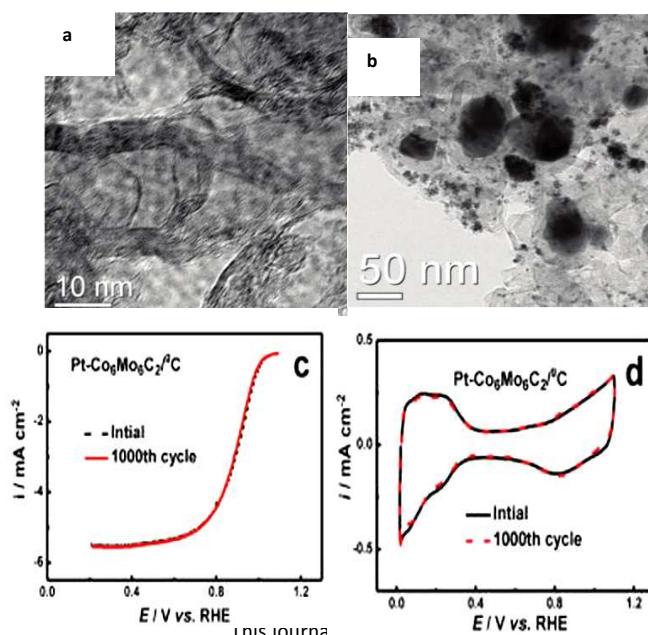


**Figure 5**(a) HRTEM image of gC, (b) TEM image of Pt-Co<sub>6</sub>Mo<sub>6</sub>C<sub>2</sub>/gC; (c) ORR curves before and after 1000 cycles on Pt-Co<sub>6</sub>Mo<sub>6</sub>C<sub>2</sub>/gC, (d) CVs before and after 1000 cycles on Pt-Co<sub>6</sub>Mo<sub>6</sub>C<sub>2</sub>/gC. Reproduced with permission from Ref. 116. Copyright the American Chemical Society 2012.

CeO<sub>2</sub> has been intensely studied for solid oxide fuel cells and catalytic applications due to its rich oxygen vacancies and low redox potential via the Ce<sup>4+</sup>/Ce<sup>3+</sup> redox cycle [117-119]. CeO<sub>2</sub> can also be a promoter to improve the ORR activity and durability of the Pt/C catalysts. Lee et al. developed an effective method to prepare highly dispersed CeO<sub>2</sub> NPs on the Pt/C catalyst [120]. In the ORR tests, the Pt-CeO<sub>2</sub>/C exhibited higher kinetic current density and positive shift of half-wave potential compare to the Pt/C catalysts. The stability of the catalytic activity was also tested by performing linear potential sweeps, and the Pt-CeO<sub>2</sub>/C showed only 20 mV degradation after 1000 cycles. On the other hand, the Pt/C catalysts showed an obvious positive shift of 72 mV in half-wave potentials. Moreover, the ECSA of Pt-CeO<sub>2</sub>/C decreased from 49 to 43 m<sup>2</sup> g<sup>-1</sup> (about 11%) after 1000 cycles, indicating no considerable decrease of Pt active surface area. While the ECSA of Pt/C decreased from 42 to 28 m<sup>2</sup> g<sup>-1</sup> (about 33%), which indicated that the Pt-CeO<sub>2</sub>/C catalyst was significantly more durable compared to the Pt/C catalyst in fuel cell conditions.

#### 4.2 Improve the activity by ordered nano-ceramic supports

Currently, highly oriented nanostructured electrodes with one-dimensional structure have attracted more attention because of significantly increased surface area and unique physicochemical properties [121-123]. For instance, Debe et al. [121] reported that the unique nanostructured thin film (NSTF) electrode consisting of oriented nano-sized crystalline organic whiskers can improve the specific activity of the catalysts as well as reduce the loss of ECSA. Among the oriented supports, TiO<sub>2</sub> nanotube (TNT) arrays has been widely used due its high stability under fuel cell operating conditions, large surface-to-volume ratio and strong the synergistic effects between the metal and the metal oxides [124-126]. The highly ordered TNT arrays with high specific surface areas are the potential supports for fuel cell catalysts (see figure 6). The hydrogenation significantly improved the electrochemical performance of TNTs when using as catalyst supports has been demonstrated. The ordered TNT electrode showed an excellent durability during ADTs [125]. The decrease of the ECSA was only 36 % after 1000 cycles compared to the 68 % for the Pt/C electrode after 800 cycles. The ordered TNT electrode also exhibited excellent power density reached 500 and 88 mW cm<sup>-2</sup>, respectively. This research could open up new opportunities for TNT materials in fuel cells as well as in other energy devices.

#### 4.3 Improve the CO and SO<sub>2</sub> poisoning resistance

Hitherto, low content of CeO<sub>2</sub> has been used to improve the CO and SO<sub>2</sub> poisoning resistance for the traditional Pt/C catalysts

[127]. Different ratio of CeO<sub>2</sub> up to 6% was introduced to the Pt/C catalyst by a moderate method. The loss of active sites for

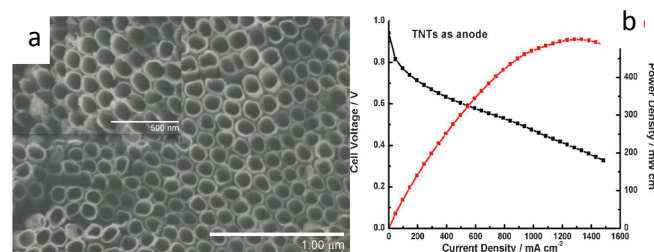


**Figure 6** (a) Field emission SEM (FESEM) images of H-TNTs annealed at 450 for 1 h (scale bar = 1 μm). Insets: Magnified FESEM images of the H-TNTs (scale bar = 500 nm); (b) Polarization curves of the MEA using Pt-Pd-H-TNT-1-450-H as the anode and Reproduced with permission from ref. 125. Copyright 2013 Wiley-VCH.

hydrogen adsorption/desorption on Pt surfaces was negligible when 2 and 4% of CeO<sub>2</sub> was present in the catalyst, resulting in almost no performance compromise. Significantly, the SO<sub>2</sub> and CO tolerance of the prepared catalysts were also measured by the CV method. Almost 50 mV negative shift of the onset potential was observed for SO<sub>2</sub> oxidation in the presence of 2 and 4 wt% CeO<sub>2</sub>, which indicates that the SO<sub>2</sub> oxidation was promoted in the presence of CeO<sub>2</sub>. Meanwhile, the enhancement towards CO oxidation was examined by the CO stripping, and the onset potential for the CO oxidation also had a negative shift with the increased CeO<sub>2</sub> amount, indicating that the high concentration of surface oxygen vacancies of the CeO<sub>2</sub> can enhance the oxygen diffusion and spillover, and hence assist the CO oxidation on Pt surfaces.

Boron carbide (B<sub>4</sub>C), as one of the most stable carbides due to its low density and high stable in acidic solution, has widely been used in wear resistant, armor and neutron absorber materials [128-130]. B<sub>4</sub>C is also expected as an alternative support for the fuel cell catalyst, because it can promote the catalytic activity through synergistic effects [131, 132]. Recently, the Pt/B<sub>4</sub>C catalyst was synthesized and showed greatly enhanced MOR activity and CO tolerance than that of Pt/C catalyst [133]. The catalyst showed a very high peak current density of 63 mA cm<sup>-2</sup>, which was nearly twice that of Pt/C catalysts (37 mA cm<sup>-2</sup>). Meanwhile, the Pt/B<sub>4</sub>C catalyst had most negative onset potential shift for the MOR and CO tolerance compared to that of the Pt/C, which could be attributed to fast hydroxyl adsorption and high OH<sub>ad</sub> coverage occurring during the hydrogen desorption process. These results suggest promising applications for the nano-B<sub>4</sub>C as next generation catalyst support for fuel cells.

NbC NWs with high electrical conductivity and outstanding resistance of oxidation, were synthesized through a bamboo-based carbon-thermal method and used as alternative supports of Pt NPs for DMFCs [134]. The Pt/NbC NWs catalysts



exhibited very high peak current density of 766.1 mA mg<sup>-1</sup> Pt, which was more than 3 times of the Pt/C (221.7 mA mg<sup>-1</sup> Pt). Meanwhile, the onset and peak potential of the Pt/NbC NWs showed a larger negative shift, which indicated that the NbC NWs supports can effectively reduce the overpotential due to the synergistic effect between the Pt NPs and supports. There was an only 2.4% loss of the peak current density for the Pt/NbC NWs after 200 linear sweeping cycles, while the Pt/C showed almost 19.4% loss after the same number of cycles. The above results indicate that the NbC NWs possesses a promising application as the catalyst supports for the DMFCs or other electrocatalytic field.

Tungsten-based nano-ceramic materials have also attracted many attentions as alternative supports for the fuel cell catalysts due to their chemical and electrochemical activities and synergistic effect for many reactions. WC and WO<sub>x</sub> can help enhance the catalytic activity for ORR and MOR, and improve the CO and sulfur tolerance [135-139]. Shen et al. firstly developed the PdFe-WC/C catalyst for the direct alcohol fuel cells (DAFCs) with the enhanced alcohol-tolerant ORR activity due to the synergistic effect between the PdFe NPs and WC supports [140]. The PdFe-WC/C exhibited an obvious positive shift in half-wave potential for ORR than that of the PdFe/C and comparative performance as that of the Pt/Cs. The effect of alcohol on the PdFe-WC/C and Pt/C as a benchmark was also performed (Figure 7). The ORR activity of the Pt/C was totally restrained because the alcohol oxidation is the dominant reaction in the presence of CH<sub>3</sub>OH or C<sub>2</sub>H<sub>5</sub>OH. In contrast, the PdFe-WC/C was hardly affected even when an alcohol concentration was up to 1.0 mol L<sup>-1</sup>. Therefore, the synergistic effect between the PdFe NPs and WC supports make the PdFe-WC/C as alternative catalysts for the ORR in the presence of alcohol and promising Pt-free cathodic catalysts for DAFCs.

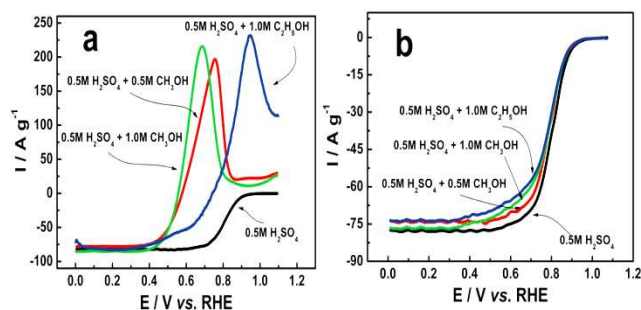


**Figure 7**(a) Pt/C and (b) PdFe-WC/C electrocatalysts in oxygen saturated 0.5 mol L<sup>-1</sup> H<sub>2</sub>SO<sub>4</sub> with or without 0.5 mol L<sup>-1</sup> CH<sub>3</sub>OH and 1.0 mol L<sup>-1</sup> CH<sub>3</sub>OH or 1.0 mol L<sup>-1</sup> C<sub>2</sub>H<sub>5</sub>OH. Rotating rate: 1600 rpm; sweep rate: 10 mV s<sup>-1</sup>; 25 °C. Reproduced with permission from ref. 140. Copyright the the Royal Society of Chemistry 2011.

Recently, WO<sub>x</sub> was adopted to modify Pt catalysts with an aim of acquiring sulfur tolerance [28]. Different ratio of WO<sub>x</sub> was introduced to the Pt/C catalyst by a moderate method. Electrochemical test results showed that the catalysts with the WO<sub>x</sub> doping exhibited the excellent sulfur tolerance than the

traditional Pt/C catalysts. The catalyst with 5 wt% WO<sub>x</sub> exhibited the best sulfur tolerance due to the synergistic effect between WO<sub>x</sub> and Pt where the OH group was generated on the hydrophilic surface of WO<sub>x</sub>, and the hydrogen spillover effect on WO<sub>x</sub> plays an important role in the oxidation of SO<sub>x</sub>. Meanwhile, the enhanced ORR activity of the WO<sub>x</sub>-Pt/C was also demonstrated by higher half-wave potential and lower amounts of H<sub>2</sub>O<sub>2</sub> formation.

Another potential approach of low-cost WC-based catalysts is that WC supports are coated by one atomic layer or monolayer (ML) of Pt metal. Chen et al. described the promising ML Pt/WC catalysts and discussed the approaches to overcoming limitations based on a better understanding of the Pt-WC interface and its behavior in electrochemical environments [141]. This perspective not only for the combination of Pt and WC, but other combinations of metals and nano-ceramic materials have great potential to be used as low-cost and stable catalysts for the fuel cell and various clean energy devices.

#### 4.4 Synergistic effect by co-catalyst function

Nano-ceramic materials also been reported that possess the ORR activity themselves and can improve the ORR activity of metal NPs after combining with metal NPs in the alkaline solution [142, 143]. Shen et al reported that the W<sub>2</sub>C nanocrystal modified Pt catalyst (Pt-W<sub>2</sub>C/C) with the enhanced ORR activity than the Pt/C. The results revealed that both of the W<sub>2</sub>C and Pt/C were active for the ORR in alkaline media. However, the overpotential of the Pt-W<sub>2</sub>C/C was significantly reduced than the P/C, which showed a synergic effect to improve the ORR activity by the co-catalyst function. The Pt-W<sub>2</sub>C/C also exhibited catalysts potential applications in anion exchange membrane hydrogen or alcohol fuel cells, alcohol monitors and metal-air batteries due to their unique properties of the selectivity and immunity to methanol. The nano-ceramic RuO<sub>2</sub> as an oxygen evolution reaction (OER) co-catalyst also has been mixed with the ORR catalyst to enhance the oxidation of water/OH<sup>-</sup> to oxygen and provide protection of other redox active species at high cathode potential. The ECSA loss of Pt catalyst was almost 100%, whereas with presence of the RuO<sub>2</sub> co-catalyst it was reduced to 30-35% [144]. Moreover, the addition of RuO<sub>2</sub>·xH<sub>2</sub>O into Pt/C catalyst increases the single cell performance but also dramatically improves the dynamic response performance, revealing that it can buffer the voltage undershoot whenever the current increases instantly [145]. The application of the co-catalyst improves the catalytic activity and the stability of the traditional catalysts, showing great potential application in fuel cells and other industrial fields.

#### 5 Summary and outlook

Carbon supports for the metal NPs catalysts are susceptible to corrosion under the harsh chemical and electrochemical oxidation conditions in fuel cells including acidic electrolyte (pH<1) and high operating potential (up to 1.2 V). The nano-ceramic materials have been considered as the alternative support materials to replace the traditional carbon supports due

to their unique mechanical properties, excellent thermal stability, and outstanding oxidation and acid corrosion resistance. This perspective has reviewed recently significant progress in using nano-ceramic materials as the supports of the low temperature fuel cell catalysts. Such novel nano-ceramic supports can improve the stability of the catalyst as expected, and simultaneously enhance its catalytic activity and CO/SO<sub>2</sub> poisoning resistance by the synergistic effects between the metal catalyst and nano-ceramic support. Although the potential application of nano-ceramic supports has been demonstrated, the practical is limited because of their low conductivity. So the future efforts should be focused on the following aspects. Firstly, to further improve the stability of the catalyst by developing more stable nano-scale ceramic supports with high specific surface area, which can increase the adsorption capability of the metal NPs on supports to get homogeneously dispersed catalysts. At the same time different shapes of nano-ceramic supports, such as nanowires and nanotubes, are also desired, not only confined to the common nano-spherical structure. For example, the highly ordered TiO<sub>2</sub> naotube arrays with high specific surface areas are the potential supports for fuel cell catalysts. Secondly, the cost reduction is important for the fuel cell industry. Enhancing the catalytic activity by the synergistic effects between the metal nanoparticles and nano-ceramic supports, and reducing the usage of Pt NPs by coating one atomic layer or ML of Pt metal on nano-ceramic supports are also the potential strategies. Thirdly, the conductivity of the nano-ceramic supports is very important for the performance of the metal catalysts, so developing the novel pure or composite metal-like nano-ceramic supports (e.g., ZrB<sub>2</sub>, ZrB<sub>2</sub>-SiC, ZrB<sub>2</sub>-B<sub>4</sub>C) with superior resistance to oxidation is the potential direction for their wide application. On the other hand, the hybrid support systems consisting of metal element doping nano-ceramic supports and combining nano-ceramic and nanocarbon supports (e.g., graphene, carbon nanotubes, nanofibres), are also the promising solutions to solve this problem. To further enhance the catalytic activity, tolerance of the harmful gases, and water management to increase volumetric specific power of the fuel cell stack, the elevated temperature fuel cell (<200 °C) is the potential trend. However, the corrosion of conventional carbon supports can be further exacerbated. Hence, the nano-ceramic materials can be an important alternative supports due to their unique mechanical properties, conductivity, and superior oxidation and acid corrosion resistance.

### Acknowledgements

This work was financially supported by the National Natural Science Foundation of China (NSFC) (51372186), the National Basic Research Development Program of China (973 Program) (No.2012CB215504), and the self-determined and innovative research funds of WUT (2012-YB-05).

### Notes and references

State Key Laboratory of Advanced Technology for Materials Synthesis and Processing, Wuhan University of Technology, Wuhan 430070, China.

- \*Corresponding author: Email: msc@whut.edu.cn. Tel.: +86 27 87651837; fax: +86 27 87879468.
- 1 J. Zhang, K. Sasaki, E. Sutter and R. R. Adzic, *Science*, 2007, 315, 220-222.
  - 2 K. Ahmed and K. Foger, *Ind. Eng. Chem. Res.*, 2010, 49, 7239-7256.
  - 3 Q. F. Li, R. H. He, J. O. Jensen and N. J. Bjerrum, *Chem. Mater.*, 2003, 15, 4896-4915.
  - 4 M. Pumera, *Energy Environ. Sci.*, 2011, 4, 668-674.
  - 5 K. S. Novoselov, A. K. Geim, S. V. Morozov, D. Jiang, M. I. Katsnelson, I. V. Grigorieva, S. V. Dubonos and A. A. Firsov, *Nature*, 2005, 438, 197-200.
  - 6 R. Wang, C. Xu, X. Bi and Y. Ding, *Energy Environ. Sci.*, 2012, 5, 5281-5286.
  - 7 M. K. Debe, *Nature*, 2012, 486, 43-51.
  - 8 Z. Chen, D. Higgins, A. Yu, L. Zhang and J. Zhang, *Energy Environ. Sci.*, 2011, 4, 3167-3192.
  - 9 K. S. Novoselov, A. K. Geim, S. V. Morozov, D. Jiang, M. I. Katsnelson, I. V. Grigorieva, S. V. Dubonos and A. A. Firsov, *Nature*, 2005, 438, 197-200.
  - 10 T. J. Schmidt, H. A. Gasteiger, G. D. Stab, P. M. Urban, D. M. Kolb and R. J. Behm, *J. Electrochem. Soc.*, 1998, 145, 2354-2358.
  - 11 H. Lee, S. E. Habas, S. K. Weskinen, D. Butcher, G. A. Somorjai and P. Yang, *Angew. Chem. Int. Ed.*, 2006, 45, 7824-7828.
  - 12 J. C. Garcia-Martinez, R. Lezutekong and R. M. Crooks, *J. Am. Chem. Soc.*, 2005, 127, 5097-5103.
  - 13 V. R. Stamenkovic, B. Mun, S. M. Arenz, K. J. J. Mayrhofer, C. A. Lucas, G. Wang, P. N. Ross and N. M. Markovic, *Nat. Mater.*, 2007, 6, 241-247.
  - 14 C. Koenigsmann, W.-P. Zhou, R. R. Adzic, E. Sutter and S. S. Wong, *Nano Lett.*, 2010, 10, 2806-2811
  - 15 P. Makowski, A. Thomas, P. Kuhn and F. Goettman, *Energy Environ. Sci.*, 2009, 2, 480-490.
  - 16 B. Loges, A. Boddien, H. Junge and M. Beller, *Angew. Chem., Int. Ed.*, 2008, 47, 3962-3965.
  - 17 J. Zhang, H. Jin, M. B. Sullivan, F. C. H. Lim and P. Wu, *J. Phys. Chem. C*, 2009, 11, 1441-1446.
  - 18 N. Tian, Z.-Y. Zhou, S.-G. Sun, Y. Ding and Z. L. Wang, *Science*, 2007, 316, 732-735.
  - 19 Y. Bing, H. Liu, L. Zhang, D. Ghosh and J. Zhang, *Chem. Soc. Rev.*, 2010, 39, 2184-2202.
  - 20 M. Yamada, S. Kon and M. Miyake, *Chem. Lett.*, 2005, 34, 1050-1051.
  - 21 S. Guo, D. Li, H. Zhu, S. Zhang, N. M. Markovic, V. R. Stamenkovic and S. Sun, *Angew. Chem. Int. Ed.*, 2013, 52, 3465-3468.
  - 22 R. Kou, Y. Y. Shao, D. H. Wang, M. H. Engelhard, J. H. Kwak, J. Wang, V. V. Viswanathan, C. M. Wang, Y. H. Lin, Y. Wang, I. A. Aksay and J. Liu, *Electrochem. Commun.*, 2009, 11, 954-957.
  - 23 S. Y. Huang, P. Ganesan and B. N. Popov, *Appl. Catal. B*, 2010, 96, 224-231.
  - 24 B. Lim, M. J. Jiang, P. H. C. Camargo, E. C. Cho, J. Tao, X. M. Lu, Y. M. Zhu and Y. N. Xia, *Science*, 2009, 324, 1302-1035.
  - 25 C. Wang, H. Daimon, T. Onodera, T. Koda and S. H. Sun, *Angew. Chem., Int. Ed.*, 2008, 47, 3588-3591.
  - 26 L. F. Dong, R. R. S. Gari, Z. Li, M. M. Craig and S. F. Hou, *Carbon*, 2010, 48, 781-787.
  - 27 A. S. Polo, M. C. Santos, R. F. B. Souza and W. A. Alves, *J. Power Sources*, 2011, 196, 872-876.

- 28 R. Xu, F. Xu, M. Pan and S.C. Mu, *RSC Advances*, 2013, 3, 764-773.
- 29 V. Mazumder, Y. M. Lee, and S.H. Sun, *Adv. Funct. Mater.*, 2010, 20, 1224-1231.
- 30 S. Zhang, Y. Y. Shao, G.P. Yin, Y.H. Lin, *J. Mater.Chem. A*, 2013, 1, 4631-4641.
- 31 E. Yoo, T. Okata, T. Akita, M. Kohyama, J. Nakamura and I. Honma, *Nano Lett.*, 2009, 9, 2255-2259.
- 32 S.J. Guo, S. Zhang and S.H. Sun, *Angew. Chem. Int. Ed.* 2013, 52, 2-21.
- 33 T. Yu, D. Y. Kim, H. Zhang, Y. Xia, *Angew. Chem.* 2011, 123, 2825-2829;
- 34 M. Gorzny, A. S. Walton and S.D. Evans, *Adv. Funct. Mater.*, 2010, 20, 1295-1300.
- 35 S. H. Sun, G. X. Zhang, D. S. Geng, Y. G. Chen, R. Y. Li, M. Cai and X. L. Sun, *Angew. Chem., Int. Ed.*, 2011, 50, 422-426.
- 36 S. J. Guo, D. G. Li, H. Y. Zhu, S. Zhang, N. M. Markovic, V. R. Stamenkovic, S. H. Sun, *Angew. Chem. Int. Ed.*, 2013, 52, 3465-3468.
- 37 C. Koenigsmann, A.C. Santulli, K.P. Gong, M.B. Vukmirovic, W.P. Zhou, E. Sutter, S.S. Wong and R.R. Adzic, *J. Am. Chem. Soc.*, 2011, 133, 9783-9795.
- 38 Y. J. Wang, D. P. Wilkinson and J. J. Zhang, *Chem. Rev.*, 2011, 111, 7625-7651.
- 39 D. P. He, K. Cheng, T. Peng, M. Pan and S. C. Mu, *J. Mater. Chem. A*, 2013, 1, 2126-2132.
- 40 H. G. Li, N. C. Cheng, Y. Zheng, X. Zhang, H. F. Lv, D. P. He, M. Pan, F. Kleitz, S. Z. Qiao and S. C. Mu, *Adv. Energy Mater.*, 2013, 3, 1176-1179.
- 41 D. C. Higgins, J. Y. Choi, J. Wu, A. Lopez and Z. W. Chen, *J. Mater. Chem.*, 2012, 22, 3727-3732.
- 42 S. Zhang, Y. Shao, H. Liao, M. H. Engelhard, G. Yin and Y. Lin, *ACS Nano*, 2011, 5, 1785-1791.
- 43 E. Yoo, T. Okata, T. Akita, M. Kohyama, J. Nakamura and I. Honma, *Nano Lett.*, 2009, 9, 2255-2259.
- 44 X. Ji, K. T. Lee, R. Holden, L. Zhang, J. Zhang, G. A. Botton, M. Couillard and L. F. Nazar, *Nat. Chem.*, 2010, 2, 286-293.
- 45 S. J. Guo and S. H. Sun, *J. Am. Chem. Soc.*, 2012, 134, 2492-2495.
- 46 E. Antolini and E.R. Gonzalez, *Solid State Ion.*, 2009, 180, 746-763.
- 47 X. Cui, J. Shi, H. Chen, L. Zhang, L. Guo, J. Gao and J. Li, *J. Phys. Chem. B*, 2008, 112, 12024-12031.
- 48 L. G. R. A. Santos, K. S. Freitas and E. A. Ticianelli, *J. Solid State Electrochem.*, 2007, 11, 1541-1548.
- 49 M.S. Hino, S. Kobayashi and K. Arata, *J. Am. Chem. Soc.*, 1979, 101, 6439-6441.
- 50 N. V. Krstajic, L. M. Vracar, V. R. Radmilovic, S. G. Neophytides, M. Labou, J. M. Jaksic, R. Tunold, P. Falaras and M. M. Jaksic, *Surf. Sci.*, 2007, 601, 1949-1966.
- 51 T. Ioroi, Z. Siroma, N. Fujiwara, S. Yamazaki and K. Yasuda, *Electrochem. Comm.*, 2005, 7, 183-188.
- 52 T. Ioroi, H. Senoh, S. Yamazaki, Z. Siroma, N. Fujiwara and K. Yasuda, *J. Electrochem. Soc.*, 2008, 155, B321-B326.
- 53 S. Andersson, B. Collen, U. Kuylenstierna and A. Magneli, *Acta Chem. Scand.* 1957, 11, 1641-1657.
- 54 S.Y. Huang, P. Ganesan, S. Park and B.N. Popov, *J. Am. Chem. Soc.* 2009, 131, 13898-13899.
- 55 Z. Liu, J. Zhang, B. Han, J. Du, T. Mu, Y. Wang and Z. Sun, *Microporous Mesoporous Mater.*, 2005, 81, 169-174.
- 56 X. Chen and S. S. Mao, *Chem. Rev.*, 2007, 107, 2891-2959.
- 57 D. S. Kim and S.-Y. Kwak, *Appl. Catal., A* 2007, 323, 110-118.
- 58 J. Zhu, B. Y. Tay and J. Ma, *Mater. Lett.*, 2006, 60, 1003-1010.
- 59 E. Antolini and E.R. Gonzalez, *Solid State Ionics.*, 2009, 180, 746-763.
- 60 T. Matsui, T. Okanishi, K. Fujiwara, K. Tsutsui, R. Kikuchi and T. Takeguchi, *Sci. Technol. Adv. Mater.*, 2006, 7, 524-530.
- 61 Y. S. Kim, H. S. Jang and W. B. Kim, *J. Mater. Chem.*, 2010, 20, 7859-7863.
- 62 K.S. Lee, I.S. Park, Y.H. Cho, D.S. Jung, N. Jung and H.Y. Park, *J. Catal.*, 2008, 258, 143-152.
- 63 D. J. You, K. Kwon, C. Pak and H. Chang, *Catal. Today.*, 2009, 146, 15-19.
- 64 P. Zhang, S.Y. Huang and B.N. Popov, *J. Electrochem. Soc.* 2010, 157, B1163-B1172.
- 65 L. Wang, D.M. Xing, Y.H. Liu, Y.H. Cai, Z.G. Shao and Y.F. Zhai, *J. Power Sources*, 2006, 161, 61-67.
- 66 S. E. Skrabalak and K. S. Suslick, *J. Am. Chem. Soc.*, 2006, 128, 12642-12643.
- 67 B. Seger, A. Kongkanand, K. Vinodgopal, P. V. Kamat, *J. Electroanal. Chem.* 2008, 621, 198-204.
- 68 P.J. Kulesza and L.R. Faulkner, *J. Electrochem. Soc.*, 1989, 136, 707-713.
- 69 L.W. Niedrach and H.I. Zeliger, *J. Electrochem. Soc.*, 1969, 116, 152-153.
- 70 E. Antolini and E.R. Gonzalez, *Appl. Catal. B*, 2010, 96, 245-266.
- 71 H. Chhina, S. Campbell and O. Kesler, *J. Electrochem. Soc.*, 2007, 154, B533-B539.
- 72 F. Micoud, F. Maillard, A. Gourgaud and M. Chatenet, *Electrochem. Commun.*, 2009, 11, 651-654.
- 73 K. W. Park, J. H. Choi, K. S. Ahn and Y. E. Sung, *J. Phys. Chem., B* 2004, 108, 5989-5994.
- 74 Y. Suzuki, A. Ishihara, S. Mitsushima, N. Kamiya and K. Ota, *Electrochem. Solid-State Lett.* 2007, 10, B105-B107.
- 75 S. E. Skrabalak and K. S. Suslick, *J. Am. Chem. Soc.*, 2006, 128, 12642-12643.
- 76 S. A. G. Evans, J. G. Terry, N. Plank, A. Walton, L. Keane, C. Campbell, P. Ghazal, J. Beattie, T. Su, J. Crain and A. Mount, *Electrochem. Comm.*, 2005, 7, 125-129.
- 77 O. T. Musthafa and S. Sampath, *Chem. Commun.*, 2008, 67-69.
- 78 J. Giner and L. Swette, *Nature*, 1966, 211, 1291-1292.
- 79 B. Avasarala, T. Murray, W. Z. Li and P. Haldar, *J Mater Chem*, 2009, 19, 1803-1805.
- 80 B. Avasarala and P. Haldar, *Int. J. Hydrogen Energy*, 2011, 36, 3965-3974.
- 81 B. Avasarala, and P. Haldar, *Electrochim Acta*, 2010, 55, 9024-9034.
- 82 F. Schulz, R. Drost, S. K. Hämäläinen and P. Liljeroth, *ACS Nano*, 2013, 7, 11121-11128.
- 83 Z. Q. Wang, Z. Q. Wu, N. Bramnik and S. Mitra, *Adv. Mater.*, 2013, DOI: 10.1002/adma.201304020
- 84 B. Basu, G.B. Raju and A.K. Suri, *Int. Mater. Rev.* 2006, 51, 352-374.
- 85 J. Y. Zhang, Z. Y. Fu and W. M. Wang, *J. Mater. Sci. Technol.*, 2005, 21, 841-844.
- 86 S. B. Yin, S. C. Mu, H. F. Lv, N. C. Cheng, M. Pan and Z. Y. Fu, *Appl. Catal. B*, 2010, 93, 233-240.

- 87 S. B. Yin, S. C. Mu, M. Pan and Z.Y. Fu, *J. Power Sources*, 2011, 196, 7931-7936.
- 88 H. E. Çamurlu and F. Maglia, *J. Eur. Cer. Soc.*, 2009, 29, 1501-1506
- 89 H. Zhang, J. Tang, L. Zhang and B. An, *Appl. Phys. Lett.*, 2008, 92, 173121 - 173121-3
- 90 P. Jash, A.W. Nicholls, R. S. Ruoff and M. Trenary, *Nano Lett.*, 2008, 8, 3794-3798
- 91 J. Y. Ju, C. H. Kim, J. J. Kim, J. H. Lee, H. S. Lee and Y. D. Shin, *J. Electr. Eng. Technol.*, 2009, 4, 538-545.
- 92 M. J. Ledoux, F. Meunier, B. Heinrich, C. Pham-Huu, M.E. Harlin and A.O.I. Krause, *Appl. Catal. A*, 1999, 181, 157-170.
- 93 T. Narushima, T. Goto and T. Hirai, *J. Am. Ceram. Soc.*, 1989, 72, 1386-1390.
- 94 J. C. Summers, S. Van Houtte and D. Psaras, *Appl. Catal. B*, 1996, 10, 139-156.
- 95 H. F. Lv, S. C. Mu, N. C. Cheng and M. Pan, *Appl. Catal., B*, 2010, 100, 190-196.
- 96 J. B. Zang, L. Dong, Y. D. Jia, H. Pan, Z. Z. Gao and Y. H. Wang, *Appl. Catal., B*, 2014, 144, 166-173.
- 97 R. Dhiman, E. Johnson, E. M. Skou, P. Morgen and S.M. Andersen, *J. Mater. Chem. A*, 2013, 1, 6030-6036.
- 98 D. Wang, J. Yang, X. Li, D. Geng, R. Li, M. Cai, T.-K. Sham, X. Sun, *Energy Environ. Sci.*, 2013, 6, 2900-2906
- 99 Y. L. Shen, S. L. Chen, J. M. Song and I. G. Chen, *Nanoscale Res Lett*, 2012, 7, 237-241.
- 100 X. Chen, and S. S. Mao, *Chem. Rev.* 2007, 107, 2891-2959.
- 101 D. S. Kim, and S. Y. Kwak, *Appl. Catal., A*, 2007, 323, 110-118.
- 102 R. Asahi, T. Morikawa, T. Ohwaki, K. Aoki and Y. Taga, *Science*, 2001, 293, 269-271.
- 103 D. Morris, Y. Dou, J. Rebane, C.E.J. Mitchell, R.G. Egdell, D.S.L. Law, A. Vittadini and M. Casarin, *Phys. Rev. B*, 2000, 61, 13445-13457.
- 104 A. Bernasik, M. Radecka, M. Rekas and M. Sloma, *Appl. Surf. Sci.*, 1993, 65-66, 240-245.
- 105 L. R. Sheppard, T. Bak, J. Nowotny and M.K. Nowotny, *Int. J. Hydrogen Energy*, 2007, 32, 2660-2663.
- 106 S. Y. Huang, P. Ganesan and B. N. Popov, *Appl. Catal. B*, 2010, 96, 224-231.
- 107 J. C. C. Fan and J. B. Goodenough, *J. Appl. Phys.*, 1977, 48, 3524-3531.
- 108 Y. Song, Y. Ma, Y. Wang, J. Di and Y. Tu, *Electrochim. Acta*, 2010, 55, 4909-4914.
- 109 O. P. Agnihotri, A. K. Sharma, B. K. Gupta and R. Thangaraj, *J. Phys. D: Appl. Phys.*, 1978, 11, 643-647.
- 110 H. Chhina, S. Campbell and O. Kesler, *J. Power Sources*, 2006, 161, 893-900.
- 111 Y. Liu and E. Mustain, *J. Am. Chem. Soc.*, 2013, 135, 530-533.
- 112 H. F. Lv, N. C. Cheng, T. Peng, M. Pan and S. C. Mu, *J. Mater. Chem.*, 2012, 22, 1135-1141.
- 113 W. L. Qu, Z. B. Wang, X.L. Sui, D. M. Gu and G. P. Yin, *Fuel Cells*, 2013, 13, 149-157.
- 114 W.L. Qu, Z.B. Wang, X.L. Sui, D.M. Gu and G.P. Yin, *Int J Hydrogen Energy*, 2012, 37, 15096-15104.
- 115 R. Kou, Y.Y. Shao, D.H. Mei, Z.M. Nie, D.H. Wang, C.G. Wang, V.V. Viswanathan, S. Park, I.A. Aksay, Y.H. Lin, Y. Wang and J. Liu, *J. Am. Chem. Soc.*, 2011, 133, 2541-2547.
- 116 X. M. Ma, H. Meng, M. Cai and P.K. Shen, *J. Am. Chem. Soc.*, 2012, 134, 1954-1957.
- 117 J. Kaspar, P. Fornasiero and M. Graziani, *Catal. Today*, 1999, 50, 285-298.
- 118 H. C. Yao and Y. F. Y. Yao, *J. Catal.*, 1984, 86, 254-265.
- 119 X.Z. hang and K. J. Klabunde, *Inorg. Chem.*, 1992, 31, 1706-1709.
- 120 D. H. Lim, W.D. Lee, D.H. Choi and H.I. Lee, *Appl. Catal. B*, 2010, 94, 85-96.
- 121 M. K. Debe, *Nature*, 2012, 486, 43-51.
- 122 S. H. Kang, Y.E. Sung and W.L. Smyrl, *J. Electrochem. Soc.*, 2008, 155, B1128-B1135.
- 123 H. C. He, P. Xiao, M. Zhou, F. L. Liu, S. J. Yu, L. Qiao and Y. H. Zhang, *Electrochim. Acta*, 2013, 88, 782-789.
- 124 C. K. Zhang, H. M. Yu, Y.K. Li, L. Fu, Y. Gao, W. Song, Z.G. Shao and B. L. Yi, *Nanoscale*, 2013, 5, 6834-6841.
- 125 C. K. Zhang, H. M. Yu, Y. K. Li, Y. Gao, Y. Zhao, W. Song, Z.G. Shao and B.L. Yi, *ChemSusChem*, 2013, 6, 659-666.
- 126 Y. Y. Song, Z. D. Gao and P. Schmuki, *Electrochem. Commun.*, 2011, 13, 290-293.
- 127 F. Xu, R. Xu and S. C. Mu, *Electrochim. Acta*, 2013, 112, 304-309.
- 128 W. Q. Han, P. Kohler-Redlich, F. Ernst and M. Ruhle, *Chem. Mater.*, 1999, 11, 3620-3623.
- 129 J. H. Morris, *Chem. Rev.*, 1985, 85, 51-76.
- 130 A. Velamakanni, K. J. Ganesh, Y. W. Zhu, P. J. Ferreira and R. S. Ruoff, *Adv. Funct. Mater.*, 2009, 19, 3926-3933.
- 131 D. W. McKee, A. J. Scarpellino, I. F. Danzig and M. S. Pak, *J. Electrochem. Soc.*, 1969, 116, 562-568.
- 132 W. T. Grubb and D. W. McKee, *Nature*, 1966, 210, 192-194.
- 133 H. F. Lv, T. Peng, P. Wu, M. Pan and S.C. Mu, *J. Mater. Chem.*, 2012, 22, 9155-9160.
- 134 Z. Qiu, H. Huang, J. Du, T. Feng, W.K. Zhang, Y.P. Gan and X.Y. Tao, *J. Phys. Chem. C*, 2013, 117, 13770-13775.
- 135 F. P. Hu, G. F. Cui, Z. D. Wei and P. K. Shen, *Electrochem. Commun.*, 2008, 10, 1303-1306.
- 136 Z. Z. Zhao, X. Fang, Y. L. Li, Y. Wang, P. K. Shen, F. Y. Xie and X. Zhang, *Electrochem. Commun.*, 2009, 11, 290-293.
- 137 M. Nie, P. K. Shen, M. Wu, Z. D. Wei and H. Meng, *J. Power Sources*, 2006, 162, 173-176.
- 138 H. Meng and P. K. Shen, *Chem. Commun.*, 2005, 35, 4408-4410.
- 139 C. A. Ma, J. F. Sheng, N. Brandon, C. Zhang and G. H. Li, *Int. J. Hydrogen Energy*, 2007, 32, 2824-2829.
- 140 S. B. Yin, M. Cai, C.X. Wang and P.K. Shen, *Energy Environ. Sci.*, 2011, 4, 558-563.
- 141 D. V. Esposito and J. G. G. Chen, *Energy Environ. Sci.*, 2011, 4, 3900-3912.
- 142 H. Meng and P.K. Shen, *Electrochem. Commun.*, 2006, 8, 588-594.
- 143 H. Meng and P.K. Shen, *Chem. Commun.*, 2005, 35, 4408-4410.
- 144 R. Srivastava and P. Strasser, *ECS Trans.*, 2009, 25, 565-571.
- 145 X. Wu, H. Xu, L. Lu, J. Fu and H. Zhao, *Int. J. Hydrogen Energy*, 2010, 35, 2127-2133.